

Nuclear-quadrupole double-resonance study of the solid solution $\text{Rb}_{1-x}\text{Tl}_x\text{H}_2\text{PO}_4$

J. Seliger and V. Žagar

J. Stefan Institute, University of Ljubljana, Jamova 39, 61000 Ljubljana, Slovenia

(Received 15 November 1994; revised manuscript received 7 February 1995)

The solid solution $\text{Rb}_{1-x}\text{Tl}_x\text{H}_2\text{PO}_4$ has been investigated by the nuclear-quadrupole double-resonance methods. The ^{87}Rb nuclear quadrupole resonance (NQR) spectrum in the solid solution $\text{Rb}_{1-x}\text{Tl}_x\text{H}_2\text{PO}_4$ exhibits for $x > 0.2$ the concentration dependences of the linewidth and of the center frequency characteristic for homogeneously mixed samples. The ^{87}Rb NQR spectra as measured in a mixed sample with a low concentration of rubidium ions ($x = 0.98$) show that the antiferroelectric phase transition in TlH_2PO_4 is associated with the condensation of two displacement waves. In a mixed sample with the concentration x of TlH_2PO_4 of 0.9, a phase transition is observed at nearly the same temperature as in TlH_2PO_4 . No phase transition is observed in the mixed crystals with the concentration x of TlH_2PO_4 between 0.2 and 0.8. The shape of the 5/2-3/2 transition line in the ^{17}O NQR transition spectrum is used for the determination of the Edwards-Anderson order parameter q_{EA} . The temperature dependences of q_{EA} in $\text{Rb}_{0.5}\text{Tl}_{0.5}\text{H}_2\text{PO}_4$ and in $\text{Rb}_{0.8}\text{Tl}_{0.2}\text{H}_2\text{PO}_4$ demonstrate that we are in both cases dealing with a random-field smearing of a random-bond-type pseudospin spin-glass transition.

I. INTRODUCTION

Some solid solutions of the KDP-type ferroelectrics and antiferroelectrics exhibit glass properties in limited concentration ranges. The most extensively studied solid solution of this type is $\text{Rb}_{1-x}(\text{NH}_4)_x\text{H}_2\text{PO}_4$ (RADP),^{1,2} which for $x < 0.22$ undergoes a ferroelectric phase transition, whereas for $x > 0.74$ it undergoes an antiferroelectric phase transition. In the intermediate-concentration range ($0.22 < x < 0.74$) RADP forms a dipolar glass. The freezing transition into the deuteron-glass phase of the deuterated compound $\text{Rb}_{1-x}(\text{ND}_4)_x\text{D}_2\text{PO}_4$ (DRADP) is, as verified by the NMR technique,³ associated with a random freezeout of the deuteron motion in the $\text{O}-\text{H}\cdots\text{O}$ hydrogen bonds. The local polarization distribution $W(p)$ and its second moment, the Edwards-Anderson order parameter in DRADP, show the characteristic features predicted by a deuteron-glass model with infinitely ranged random-bond interactions in the presence of quenched random fields.⁴ The slowing down of the proton or deuteron motion in RADP and DRADP which occurs on cooling into the glass phase affects the deuterium and rubidium quadrupole-perturbed NMR line shapes at relatively low temperatures. On the other hand, the Tl^{2+} line shapes and second moments in Tl-doped RADP allow for a direct determination of the static and dynamic features of the glass transition in RADP.⁵

The solid solution $\text{K}_{1-x}(\text{NH}_4)_x\text{H}_2\text{PO}_4$ (KADP) is analogous to RADP, but it is much less studied. The vanishing of the ferroelectric phase transition is in KADP observed when $x > 0.2$, whereas the antiferroelectric phase transition vanishes when $x < 0.85$.⁶ In the intermediate-concentration range, the dielectric measure-

ments show a low-frequency dispersion of the dielectric constant characteristic for a glassy system.⁷ A similar low-frequency dispersion of the dielectric constant was observed also in glassy RADP.¹

A solid solution of ferroelectric RbH_2PO_4 (RDP) and antiferroelectric TlH_2PO_4 (TIDP) also represents a compound in which the random distribution of Tl^+ and Rb^+ ions may produce a competition of the ferroelectric and antiferroelectric structures and, in a certain concentration range, also frustration and formation of a dipolar glass.

TIDP is known to undergo an antiferroelectric phase transition at $T_c = 203$ K. It is, in contrast to tetragonal KDP, ADP, and RDP, monoclinic in the paraelectric phase, which is presumably the effect of a larger Tl^+ ionic radius as compared to the ionic radii of K^+ , NH_4^+ , Rb^+ . In the paraelectric phase, two out of the four $\text{O}-\text{H}\cdots\text{O}$ hydrogen bonds linking a PO_4 group to four other PO_4 groups are symmetric, whereas the other two $\text{O}-\text{H}\cdots\text{O}$ hydrogen bonds are weakly asymmetric.⁸⁻¹⁰ On going below T_c , the two previously symmetric hydrogen bonds become asymmetric, which is presumably, as in other compounds of the KDP family, the effect of the freeze out of the hydrogen motion between two equivalent equilibrium sites in an $\text{O}-\text{H}\cdots\text{O}$ hydrogen bond. Also the hydrogen bonds which are asymmetric above T_c become more asymmetric below T_c in the antiferroelectric phase.¹⁰

In paraelectric RDP a PO_4 group is linked to four other PO_4 groups by four equivalent symmetric $\text{O}-\text{H}\cdots\text{O}$ hydrogen bonds.¹¹ On decreasing the temperature, RDP transforms into the ferroelectric phase at $T_c = 147$ K. In the ferroelectric phase, the four $\text{O}-\text{H}\cdots\text{O}$ hydrogen bonds become asymmetric, but they remain equiv-

alent.^{11,12} The asymmetry of the O—H . . . O hydrogen bonds is, in ferroelectric RDP, the effect of the freeze out of the hydrogen motion between two equivalent equilibrium sites O—H . . . O and O . . . H—O. There are some other features in RDP which seem to be associated with the size of a Rb⁺ ion. On deuteration, which slightly increases the lengths of the hydrogen bonds [$R(\text{O—D} \cdots \text{O}) > R(\text{O—H} \cdots \text{O})$], the crystal structure transforms from tetragonal to monoclinic.^{13,14} When the tetragonal RDP is heated above 84 °C, a phase transition occurs into the high-temperature monoclinic phase.¹⁵ The monoclinic high-temperature phase of RDP can easily be supercooled to room temperature or even to lower temperatures where it slowly transforms into the stable tetragonal phase.¹⁶

A partial substitution of rubidium ions by thallium ions is expected to affect the sensitive network of the O—H . . . O hydrogen bonds. The structure and properties of the mixed compound Rb_{1-x}Tl_xH₂PO₄ (RTIDP) are thus expected to be significantly different from the structures and properties of the pure compounds RDP and TIDP.

Nuclear-quadrupole resonance (NQR) represents a sensitive technique for the study of structural changes caused by the partial substitution of cations. In RTIDP there are two nuclear species ⁸⁷Rb and ¹⁷O, which may give useful information on the structure of the mixed compound. There are also ⁸⁵Rb nuclei present which are even more abundant than ⁸⁷Rb nuclei. But the nuclear magnetic moment of a ⁸⁵Rb nucleus is significantly lower than the nuclear magnetic moment of a ⁸⁷Rb nucleus and in mixed compounds the ⁸⁵Rb NQR lines which in fact overlap with the ⁸⁷Rb NQR lines strongly broaden. By an appropriate choice of the experimental technique, we can get rid of the weak ⁸⁵Rb NQR signals.

A ⁸⁷Rb nucleus represents in RTIDP a nonlocal probe. A Rb⁺ ion is ionically bonded to the surrounding ions and the electric-field-gradient (EFG) tensor at the site of its nucleus represents the sum of the contributions of a large number of surrounding ions. An ¹⁷O nucleus represents, on the other hand, a local probe. The EFG tensor at its site is mainly determined by the electric charge distribution in the covalent and hydrogen bonds formed by the oxygen atom. ¹⁷O NQR is thus expected to give valuable information on the local polarization distribution in RTIDP.

In the present paper, we present the results of the ⁸⁷Rb and ¹⁷O NQR study of the solid solution Rb_{1-x}Tl_xH₂PO₄ for $x = 0.98, 0.9, 0.8, 0.5,$ and 0.2 . Both NQR spectra are measured by a highly sensitive nuclear-quadrupole double-resonance technique. The ⁸⁷Rb NQR spectra are compared to the ⁸⁷Rb quadrupole-perturbed NMR spectra in RADP. The Edwards-Anderson order parameter q_{EA} is calculated from the ¹⁷O NQR spectra and analyzed in the random-bond random-field model.

II. EXPERIMENTAL DETAILS

⁸⁷Rb has a spin $\frac{3}{2}$ and thus two doubly degenerated quadrupole energy levels in zero magnetic field with the resonance, NQR, frequency ν_Q being

$$\nu_Q = (eQV_{ZZ}/2h)(1 + \eta^2/3)^{1/2}. \quad (1)$$

Here eQV_{ZZ}/h is the quadrupole coupling constant and η is the asymmetry parameter of the EFG tensor at the site of the nucleus. Crystallographically in inequivalent sites of ⁸⁷Rb generally differ in both the quadrupole coupling constant as well as in the asymmetry parameter η . They are thus characterized by different NQR frequencies.

¹⁷O has a spin $\frac{5}{2}$. It has thus in zero magnetic field three doubly degenerated nuclear-quadrupole energy levels. The energies of the nuclear-quadrupole energy levels are the solutions X of the secular equation

$$X^3 - 7(3 + \eta^2)X - 20(1 - \eta^2) = 0, \quad (2)$$

multiplied by $eQV_{ZZ}/40$. None of the three transitions between the quadrupole energy levels is, except for $\eta = 0$, forbidden and the three NQR frequencies are named as

$$\nu_{5/2-1/2} > \nu_{5/2-3/2} \geq \nu_{3/2-1/2}. \quad (3)$$

In a symmetric O—H . . . O hydrogen bond, the two oxygen sites are equivalent and only three ¹⁷O NQR frequencies are observed, whereas in an asymmetric hydrogen bond the two oxygen sites are inequivalent and two sets of three ¹⁷O NQR frequencies are observed.

The ¹⁷O and ⁸⁷Rb NQR spectra were measured by a highly sensitive nuclear-quadrupole double-resonance technique based on magnetic field cycling.^{17,18} Within a magnetic field cycle, the proton spin system is first polarized in a high static external magnetic field B_0 . Then the external magnetic field is adiabatically reduced to zero. After a time τ , the external magnetic field is adiabatically increased to the initial value B_0 and the proton NMR signal S_H is measured. It is proportional to the remaining proton magnetization and decreases with increasing τ as $S_H \sim \exp[-\tau/T_{1H}(0)]$. Here $T_{1H}(0)$ is the proton spin-lattice relaxation time in zero magnetic field. In an actual experiment, τ is chosen as being approximately equal to $T_{1H}(0)$. During the time τ spent in zero magnetic field, the sample is irradiated by a strong rf magnetic field which undergoes 180° phase shifts approximately every millisecond. The magnetic field cycles are repeated at different frequencies ν of the rf magnetic field. In resonance, i.e., when ν is equal to a NQR frequency ν_Q , the rf magnetic field induces a small splitting of the quadrupole energy levels comparable to the proton linewidth. The two spin systems resonantly couple. The 180° phase shifts of the rf magnetic field invert the populations of the two closely split energy levels of the quadrupole nuclei and thus keep the spin temperature of the quadrupole spin system high. Thus, in addition to the spin-lattice interaction, the protons are relaxed also by the interaction to “hot” quadrupole nuclei when $\nu = \nu_Q$. As a result of this additional relaxation, the proton NMR signal S_H at the end of the magnetic field cycle decreases. Thus, in the ν dependence of S_H , a dip is observed always when $\nu = \nu_Q$.

In measurements of the ¹⁷O NQR spectra, the high static magnetic field B_0 was approximately 0.8 T ($\nu_H = 32$ MHz) and magnetic field cycling was performed between

B_0 and zero magnetic field. The residence time τ in zero magnetic field was 0.4 s and during the stay in zero magnetic field the sample was irradiated by a rf magnetic field of an amplitude of approximately 2 mT. The frequency of the 180°-phase shifts of the rf magnetic field was 1.4 kHz.

The measurements of the ^{87}Rb NQR spectra were performed under the same experimental conditions as the measurements of the ^{17}O NQR spectra with the only difference being the low magnetic field within a magnetic field cycle. In the case of ^{87}Rb , the external magnetic field was cycled between B_0 and 1.5 mT and not between B_0 and zero magnetic field as in case of ^{17}O . The nonzero external magnetic field which is present during the rf irradiation strongly reduces the double-resonance signal especially when the nuclear magnetic moment of a quadrupole nucleus is low. In such a way, the double-resonance signals of ^{85}Rb are strongly reduced with respect to the double-resonance signals of ^{87}Rb .

Mixed polycrystalline RTIDP compounds were obtained by slow evaporation of water from appropriate aqueous solutions of RDP and TIDP at room temperature. The concentration x of TIDP will in the following mean the molar concentration of TIDP with respect to RDP in the aqueous solution prior to crystallization.

III. RESULTS AND DISCUSSION

A. ^{87}Rb NQR

The temperature dependence of the ^{87}Rb NQR line in RTIDP-50 ($\text{Rb}_{1-x}\text{Ti}_x\text{H}_2\text{PO}_4$, $x = 50\%$) is shown in Fig. 1. The width at the half-height of the NQR line continuously varies from approximately 1.1 MHz at room temperature to approximately 1.5 MHz at -123°C . The center frequency of the NQR line slowly increases with decreasing temperature at a rate $d\nu/dT = -1.4 \times 10^{-4}$

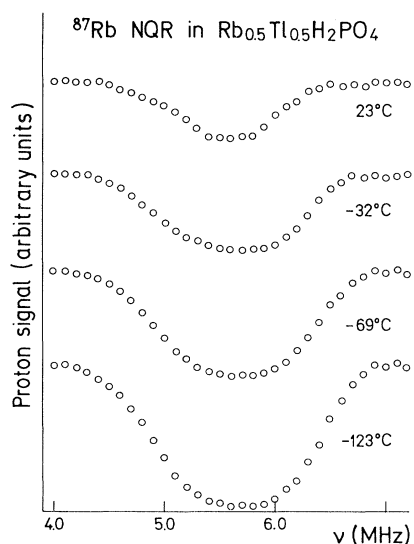


FIG. 1. Temperature dependence of the ^{87}Rb NQR line in RTIDP-50.

K^{-1} . The width of the ^{87}Rb NQR line in RTIDP-50 is much larger than the width of the ^{87}Rb NQR line in RDP, which is, when measured by the same double-resonance technique, approximately equal to 60 kHz.¹² Such a broad ^{87}Rb NQR line in RTIDP-50 may in principle be the effect of a distribution of the ^{87}Rb NQR frequencies or the effect of a slow motion which affects the rubidium EFG tensor. The slow motion would, via the dipole-dipole interaction, cause also a fast spin-lattice relaxation of the proton spin system at low magnetic fields, which was in our experiments not observed. The ^{87}Rb NQR line in RTIDP-50 thus represents a distribution of the ^{87}Rb NQR frequencies. The ^{87}Rb NQR line in RTIDP-50 has in addition no structure which would indicate the phase segregation. We may thus conclude that the sample indeed represents a homogeneous mixture of RDP and TIDP in which Rb^+ and Ti^+ ions are randomly distributed over the cation sites. The NQR frequency of a ^{87}Rb nucleus depends on the local distribution of the rubidium and thallium ions in its vicinity and varies from about 5 MHz, which is characteristic for pure RDP, to about 6 MHz, which presumably represents a rubidium ion surrounded by thallium ions (a rubidium impurity in TIDP).

The concentration dependence of the width and center frequency of the ^{87}Rb NQR line in RTIDP at room temperature is shown in Fig. 2. Here x represents the molar concentration of TIDP in an aqueous solution prior to crystallization. The present results may be compared to the results of Korner and Kind¹⁹ obtained by a quadrupole-perturbed NMR study of RADP. They obtained a linear dependence of the average ^{87}Rb quadrupole coupling constant on the concentration x of ADP in solid solution RADP. The width of the distribution of the ^{87}Rb quadrupole coupling constant was observed in RADP as being proportional to $[x(1-x)]^{1/2}$ in accor-

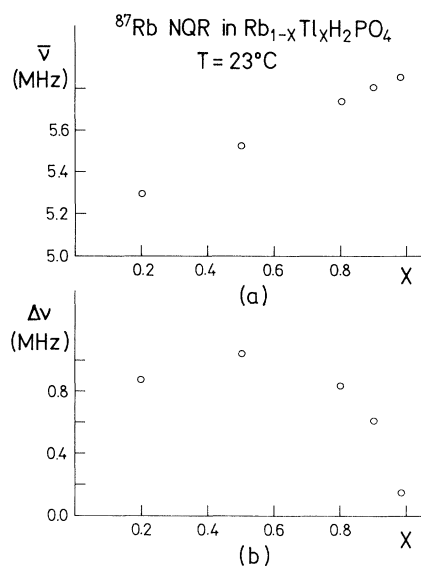


FIG. 2. Concentration dependence of the (a) center and (b) width of the ^{87}Rb NQR line in $\text{Rb}_{1-x}\text{Ti}_x\text{H}_2\text{PO}_4$ at room temperature.

dance with Kind, Blinc, and Koren.²⁰ If we assume that similar concentration dependences occur also in RTIDP, then the average ^{87}Rb NQR frequency, which is proportional to the ^{87}Rb quadrupole coupling constant and has a minor dependence on the asymmetry parameter η [expression (1)], is expected to be approximately a linear function of the concentration x of TIDP in the solid solution RTIDP. Also the width of the distribution of the ^{87}Rb NQR frequencies is expected to be approximately proportional to $[x(1-x)]^{1/2}$. From Fig. 2(a) it is clearly seen that the average ^{87}Rb NQR frequencies in the solid solutions obtained from the aqueous solutions with the concentrations x equal to 0.2, 0.5, 0.8, 0.9, and 0.98 are lying approximately on a straight line which for $x=0$ does not terminate at the ^{87}Rb NQR frequency in RDP (5.0 MHz). In the sample of RTIDP-10, a relatively narrow ^{87}Rb NQR line was observed at 5.0 MHz, but the signal-to-noise ratio was at room temperature rather poor. As will be discussed later, this is the effect of phase segregation, which occurs in this system during the crystallization process. Also the concentration dependence of the linewidth is for $x > 0.2$ in accordance with the $[x(1-x)]^{1/2}$ rule. Thus for $x > 0.2$ the mixed crystals indeed grow from an aqueous solution at room temperature and the concentration x of TIDP in the solid solution seems to be approximately equal to the concentration x of TIDP in the aqueous solution. The concentration dependence of the center and width of the NQR line is consistent with a random distribution of rubidium and thallium ions over the cation sites.

Next it is interesting to see how the partial substitution of cations influences the phase transitions. For this reason we measured the temperature dependences of the ^{87}Rb NQR spectra in samples with different concentrations x .

The temperature dependence of the ^{87}Rb NQR frequencies in RTIDP-98 is shown in Fig. 3. At room tem-

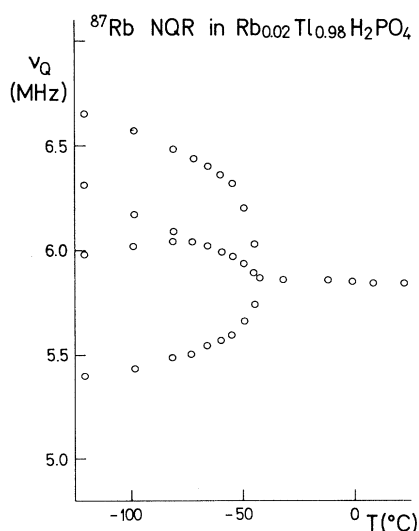


FIG. 3. Temperature dependence of the ^{87}Rb NQR frequencies in RTIDP-98.

perature a single ^{87}Rb NQR line is observed at the frequency 5.84 MHz. This frequency is significantly higher than the ^{87}Rb NQR frequency in RDP at room temperature which is equal to 5.0 MHz. Since in the mixed sample the concentration of rubidium ions is low, we may assume that a rubidium ion probes the EFG tensor at the thallium site in TIDP. Below -43°C , which is the temperature of the antiferroelectric phase transition in TIDP, the single NQR line splits into a quartet. Four crystallographically inequivalent rubidium sites and, by analogy, also four crystallographically inequivalent thallium sites are observed in antiferroelectric TIDP. A single thallium crystallographic site in the paraelectric phase agrees with x-ray⁸ and neutron scattering⁹ data which show the presence of four crystallographically equivalent thallium sites in the unit cell. The crystal structure of TIDP in the antiferroelectric phase has not yet been determined, but the present NQR results agree with the neutron scattering data of Nelmes,²¹ which show that the volume of the primitive cell doubles on cooling through T_c .

Two EFG tensors seem to be strongly affected by the phase transition, whereas the other two, represented by intermediate lines in the ^{87}Rb NQR spectra below T_c , seem to be less affected. Close to T_c the inner two lines are not separated within the experimental resolution. In a simple local model,²² where (i) the change of an EFG tensor elements is in the first approximation a linear function of the displacement of a rubidium ion from its paraelectric position and (ii) the displacements of rubidium ions from their paraelectric position are lying on one or more sinusoidal curves and which gave reasonable results in ionic incommensurate solids, we may analyze the low-temperature NQR spectra. The NQR spectra definitely show that there are two rubidium ions which displace from their paraelectric positions for, say, $+u$ and $-u$ (outer NQR lines) and two rubidium ions which in the first approximation do not displace from their paraelectric positions (inner NQR lines). If the phase transition is the result of the cell multiplication along a single axis, then the NQR results would be in accordance with the quadrupling of the unit cell. If, on the other hand, we assume that the phase transition is associated with two equivalent sinusoidal modulations in two separate directions, then the displacements $+u$ and $-u$ associated with the first modulation and the displacements $+u$ and $-u$ associated with the second modulation sum into displacements $2u$, 0 , 0 , and $-2u$, which is again in accordance with the NQR data. Neutron diffraction data²¹ seem to favor the later model.

The temperature dependence of the ^{87}Rb NQR spectra in RTIDP-90 is shown in Fig. 4. Above -43°C there is still a single ^{87}Rb NQR line at approximately 5.85 MHz, whereas below -43°C the single NQR line splits into two broad lines. There is no strong central line as in RTIDP-98. The frequency range in which the NQR frequencies are distributed below T_c agrees with the frequency range in which the four ^{87}Rb NQR frequencies are observed in RTIDP-98. The substitution of 10% of thallium ions by rubidium ions thus still does not change the structure of TIDP significantly. The mixed sample still undergoes a phase transition at nearly the same tem-

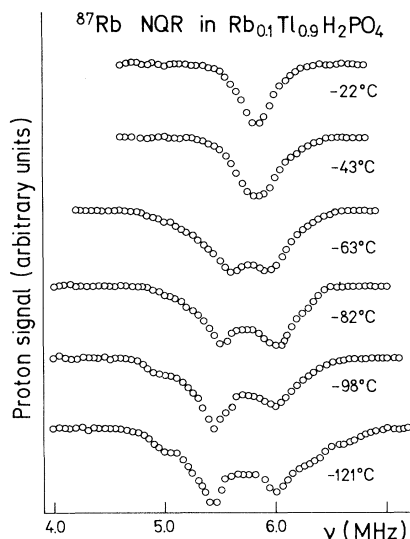


FIG. 4. Temperature dependence of the ^{87}Rb NQR spectrum in RTIDP-90.

perature as TIDP, and the difference in the NQR spectra of RTIDP-98 and RTIDP-90 seems to be a consequence of the distribution of the EFG tensors caused by the random distribution of rubidium ions.

The temperature dependence of the ^{87}Rb NQR spectra in RTIDP-80 is shown in Fig. 5. A broad NQR line is observed with the width continuously varying from 800 kHz at room temperature to 900 kHz at -121°C and with the center frequency continuously varying from 5.75 MHz at room temperature to 5.85 MHz at -121°C . No phase transition is observed in this temperature range.

In RTIDP-50 (Fig. 1), a symmetric ^{87}Rb NQR line is observed with the width continuously varying from 1.1 MHz at room temperature to 1.5 MHz at -123°C and

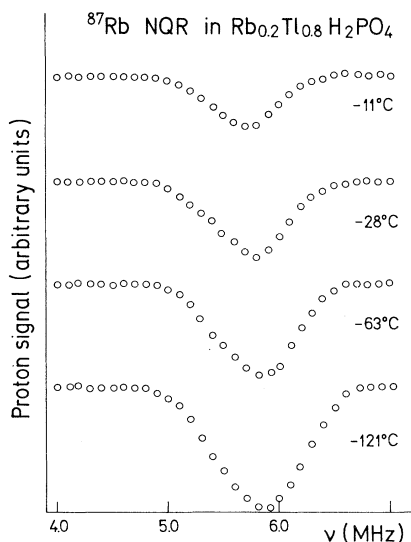


FIG. 5. Temperature dependence of the ^{87}Rb NQR spectrum in RTIDP-80.

with the center frequency continuously varying from 5.54 MHz at room temperature to 5.66 MHz at -123°C . No phase transition is observed in this temperature range.

In RTIDP-20 a nearly symmetric NQR line was observed with the width continuously varying from 850 kHz at room temperature to 950 kHz at -130°C and with the center frequency continuously varying from 5.30 MHz at room temperature to 5.45 MHz at -130°C . No phase transition was observed in this temperature range.

The temperature dependence of the ^{87}Rb NQR spectra in RTIDP-10 is shown in Fig. 6. The spectra consists of two lines: a relatively sharp line at exactly the ^{87}Rb NQR frequency in RDP and of a weaker and broader line at a somewhat higher frequency. The weaker line is definitely not the ^{85}Rb NQR line corresponding to the $\frac{5}{2}-\frac{3}{2}$ transition, which is expected to be found at about 6 MHz. A reasonable explanation of the NQR data is that during the crystallization process some crystals of pure RDP and some mixed crystals grow. This is presumably the effect of a larger ionic radius of a thallium ion as compared to the ionic radius of a rubidium ion. Thus a smaller rubidium ion can during the process of the crystal growth exchange a larger thallium ion at an arbitrary low concentration of the rubidium ions in the solution. On the other hand, a larger thallium ion cannot simply replace a smaller rubidium ion in the RDP structure. Thus a large enough concentration of thallium ions is needed in the aqueous solution in order to enter the crystal. Thus, presumably during the crystallization from the aqueous solution of 90 mol % of RDP and 10 mol % of TIDP, first the pure RDP crystals precipitate. During this process, the relative concentration of TIDP increases and the relative concentration of RDP decreases until at a high enough concentration ratio of TIDP versus RDP the mixed crystals start to grow. This critical concentration of TIDP is between 10% and 20%. The sample we measured contained both RDP and mixed crystals.

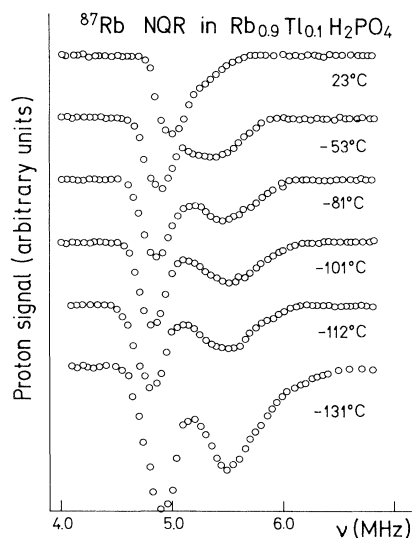


FIG. 6. Temperature dependence of the ^{87}Rb NQR spectrum in RTIDP-10.

B. ^{17}O NQR

The symmetry and order parameter of a disordered $\text{O—H}\cdots\text{O}$ hydrogen bond can be successfully studied by ^{17}O NQR. In the case of a symmetric hydrogen bond in a KDP-type system with an $\text{O—H}\cdots\text{O}$ distance of approximately 0.25 nm, the three ^{17}O NQR frequencies are approximately $\nu_{3/2-1/2}=0.98$ MHz, $\nu_{5/2-3/2}=1.49$ MHz, and $\nu_{5/2-1/2}=2.47$ MHz.^{10,12,23-26} When the bond becomes asymmetric, each of the three NQR lines splits into a doublet: a broad line corresponding to the $^{17}\text{O—H}\cdots\text{O}$ sites and a narrow line corresponding to the $\text{O—H}\cdots^{17}\text{O}$ sites. In particular, the intermediate-frequency ($\frac{5}{2}-\frac{3}{2}$) line splits into a broad line, which is in the case of complete ordering centered at approximately 1.67 MHz, and into a narrow line, which is in the case of complete ordering centered at approximately 1.39 MHz.

The part of the ^{17}O NQR spectra of pure RDP corresponding to the $\frac{5}{2}-\frac{3}{2}$ transition is, above and below T_c , shown in Fig. 7(a). A single line centered at 1.49 MHz splits below T_c into two lines. At -133°C a narrow line is observed at 1.40 MHz ($^{17}\text{O}\cdots\text{H}$ site) and a broad line at 1.62 MHz ($^{17}\text{O—H}$ site). At this temperature a proton is still moving between two inequivalent equilibrium sites in an $\text{O—H}\cdots\text{O}$ hydrogen bond at a rate which is high on the NQR frequency scale.¹² If we define the order parameter p of an $\text{O—H}\cdots\text{O}$ hydrogen bond as

$$p = P(\text{O—H}) - P(\text{O}\cdots\text{H}), \quad (4)$$

where $P(\text{O—H})$ is the probability of finding a proton at the close (O—H) position and $P(\text{O}\cdots\text{H})$ is the probability of finding a proton at the distant ($\text{O}\cdots\text{H}$) position, then the ^{17}O NQR frequencies $\nu_{5/2-3/2}$ at the close and distant positions read

$$\begin{aligned} \nu_{5/2-3/2}(\text{O—H}) &= \nu_0 + \nu_1 p + \nu_2 p^2 + \dots, \\ \nu_{5/2-3/2}(\text{O}\cdots\text{H}) &= \nu_0 - \nu_1 p + \nu_2 p^2 - \dots. \end{aligned} \quad (5)$$

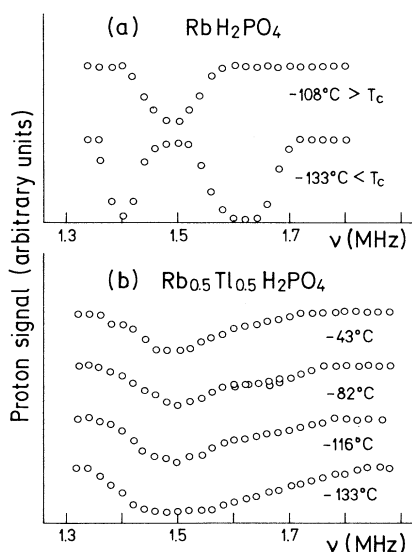


FIG. 7. ^{17}O NQR spectra in paraelectric and ferroelectric (a) RbH_2PO_4 and (b) RTIDP-50.

Here $\nu_0=1.49$ MHz, $\nu_1=140$ kHz, $\nu_2=40$ kHz, and the higher-order terms can be neglected within the experimental resolution. At -133°C the order parameter p is thus equal to 0.76.

The part of the ^{17}O NQR spectrum of RTIDP-50 corresponding to the $\frac{5}{2}-\frac{3}{2}$ transition is for the four temperatures shown in Fig. 7(b). The ^{17}O NQR spectrum of the mixed compound evidently shows the distribution of the order parameter p . On decreasing the temperature, the ^{17}O NQR spectrum of the mixed compound continuously changes. It becomes weaker at 1.5 MHz (symmetric bonds) and stronger at the positions corresponding to the asymmetric bonds. Thus the order-parameter distribution function $W(p)$ broadens. We are interested in the second moment $\langle p^2 \rangle$ of $W(p)$, which is in fact the Edwards-Anderson order parameter. We assume that $W(p)$ is a symmetric function of p , which is in fact observed in proton and deuteron glasses. Then the ensemble-averaged $\frac{5}{2}-\frac{3}{2}$ transition frequency $\langle \nu_{5/2-3/2} \rangle$ is expressed as

$$\langle \nu_{5/2-3/2} \rangle = \nu_0 + \nu_2 \langle p^2 \rangle. \quad (6)$$

The second moment M_2 of the inhomogeneously broadened NQR line,

$$\begin{aligned} M_2 &= \langle (\nu_{5/2-3/2} - \langle \nu_{5/2-3/2} \rangle)^2 \rangle \\ &= \nu_1^2 \langle p^2 \rangle + \nu_2^2 (\langle p^4 \rangle - \langle p^2 \rangle^2), \end{aligned} \quad (7)$$

is mainly determined by the first term $\nu_1^2 \langle p^2 \rangle$. The ratio $(\nu_2/\nu_1)^2$ is approximately 0.08 and $\langle p^2 \rangle$ is expected to be larger than $(\langle p^4 \rangle - \langle p^2 \rangle^2)$. We therefore neglect the second term in the expression (7). The Edwards-Anderson order parameter $q_{\text{EA}} = \langle p^2 \rangle$ can thus be determined either from the first moment [expression (6)] or from the second moment [expression (7)] of the NQR line. A more accurate determination is expected from the second moment M_2 , which depends on the term ν_1 in the expansion of the NQR frequency in powers of the order parameter p .

The second moment M_2 of the ^{17}O $\frac{5}{2}-\frac{3}{2}$ transition line is in paraelectric RDP equal to 1300 kHz^2 .² It is mainly determined by the rather strong proton-oxygen dipole-dipole interaction. At -133°C the second moment M_2 is in RDP equal to 12 500 kHz^2 . This experimentally obtained value agrees with the order parameter p of 0.76 and with the additional dipolar broadening of approximately 1300 kHz^2 . Thus, in the case of a complete ordering, the second moment of approximately 21 000 kHz^2 is expected. Since the dipolar contribution to the second moment of the NQR line only slightly varies with temperature, we can determine the Edwards-Anderson order parameter q_{EA} from the second moment M_2 of the NQR line is

$$q_{\text{EA}} = [M_2 - (1300 \text{ kHz}^2)] / (19 700 \text{ kHz}^2). \quad (8)$$

Here 1300 kHz^2 represents the dipolar contribution to the second moment M_2 of the NQR line which has to be subtracted from the second moment. The temperature dependence of the Edwards-Anderson order parameter q_{EA} as determined from the second moment M_2 of the

^{17}O $\frac{5}{2}$ - $\frac{3}{2}$ NQR line in RTIDP-50 varies from 0.27 at -43°C to 0.55 at -133°C .

The part of the ^{17}O NQR spectra showing the $\frac{5}{2}$ - $\frac{3}{2}$ transition line in RTIDP-20 is shown as a function of temperature in Fig. 8. The Edwards-Anderson order parameter as obtained by ^{17}O NQR varies from 0.28 at -31°C to 0.55 at -132°C . The temperature dependence of the Edwards-Anderson order parameter q_{EA} is presented for both RTIDP-50 and RTIDP-20, in Fig. 9. An equal value of q_{EA} is within the experimental accuracy obtained in both samples. The temperature dependence of q_{EA} is analyzed in the random-bond random-field model of Pirc, Tadić, and Blinc⁴ where $q = q_{\text{EA}}$ is the solution of the self-consistency equation

$$q = (2\pi)^{-1/2} \int_{-\infty}^{+\infty} dz e^{-z^2/2} \tanh^2[\beta \bar{J}(q + \bar{\Delta})^{1/2} z]. \quad (9)$$

Here $\beta = 1/k_B T$, $\bar{J} = T_g$ is the nominal freezing temperature, $\bar{\Delta} = \Delta/\bar{J}^2$, and Δ is the variance of the Gaussian distribution of the random fields. The best fit of the experimental data is obtained when $\bar{\Delta} = 0.4$ and $T_g = 210$ K. The theoretical temperature dependence of q_{EA} as calculated from expression (9) is shown in Fig. 9. The value of $\bar{\Delta}$ as obtained in RTIDP-50 and RTIDP-20 is comparable to the value $\bar{\Delta} = 0.35$ as obtained in DRADP,³ but it significantly differs from the value $\bar{\Delta} = 4$ as obtained in RADP.⁵ The nominal pseudo-spin-glass temperature $T_g = 210$ K in RTIDP is higher than the value $T_g = 90$ K as obtained in DRADP and $T_g = 30$ K as obtained in RADP.

IV. CONCLUSIONS

The ^{87}Rb and ^{17}O NQR spectra have been measured in polycrystalline samples of RTIDP- X ($\text{Rb}_{1-x}\text{Tl}_x\text{H}_2\text{PO}_4$, $X = 100x$) obtained by slow evaporation of water at room

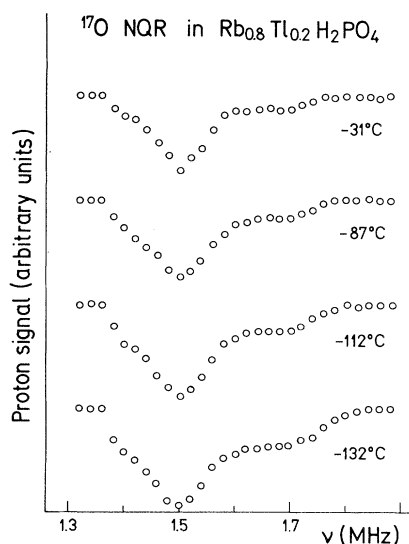


FIG. 8. Temperature dependence of the ^{17}O NQR spectrum in RTIDP-20.

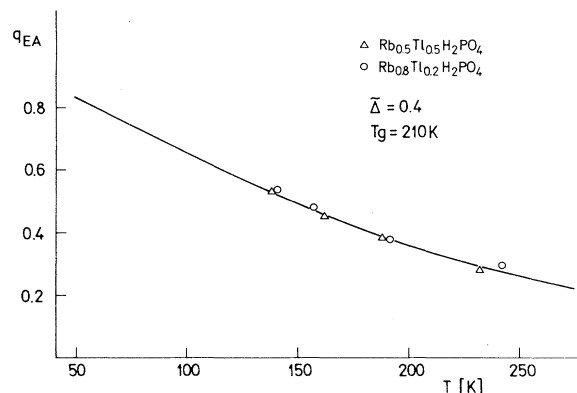


FIG. 9. Temperature dependence of the Edwards-Anderson order parameter q_{EA} in RTIDP-50 (Δ) and RTIDP-20 (\circ). The solid line represents the theoretical temperature dependence of q_{EA} as calculated from Eq. (9) with the parameters $\bar{\Delta} = 0.4$ and $T_g = 210$ K.

temperature from the aqueous solution of appropriate amounts of RDP and TIDP. In RTIDP-98 and RTIDP-90, the phase transitions were observed at approximately $T_c = -43^\circ\text{C}$, i.e., at the temperature of the phase transition in TIDP. In RTIDP-98 a single ^{87}Rb NQR line observed above T_c splits below T_c into a quartet. Close to T_c the inner two lines of the quartet are nearly not separated. We may assume that at such a low concentration of rubidium ions a rubidium ion represents an impurity which probes the structure of TIDP. When analyzed in a simple linear model, the ^{87}Rb NQR spectra show the presence of two displacement waves which freeze out below T_c . This result seems to be in agreement with the neutron scattering data.

In RTIDP- X , $X = 98, 90, 80, 50$, and 20 , the center of the distribution of the ^{87}Rb NQR frequencies depends linearly on the concentration x of TIDP in the aqueous solution prior to crystallization. Also the width of the distribution of the ^{87}Rb NQR frequencies is proportional to $[x(1-x)]^{1/2}$. A comparison of these concentration dependences to similar concentration dependences in RADP shows that homogeneously mixed crystals indeed grow from aqueous solutions of RDP and TIDP and that the concentration x of TIDP in the solid solution RTIDP is approximately equal to the concentration x of TIDP in the aqueous solution prior to crystallization.

In polycrystalline samples obtained from the aqueous solution of 10 mol % of TIDP and 90 mol % of RDP, the ^{87}Rb NQR measurements show the presence of pure RDP and the solid solution RTIDP. Phase segregation seems to occur during the crystallization process when at a too low concentration of TIDP only the crystals of RDP grow. Because of the growth of the RDP crystals, the relative concentration of TIDP in the solution increases, and when it reaches the critical value, which is somewhere between 10 and 20 mol %, the mixed crystals start to grow. This critical concentration of TIDP seems to be associated with the size of a thallium ion as compared to the size of a rubidium ion.

The ^{17}O NQR spectra in RTIDP-50 and RTIDP-20 show a distribution of the order parameters of randomly

disordered O—H · · · O hydrogen bonds. The Edwards-Anderson order parameter q_{EA} is calculated from the second moment of the ^{17}O $\frac{5}{2}$ - $\frac{3}{2}$ NQR line. Equal values of q_{EA} are obtained in both RTIDP-50 and RTIDP-20. The temperature dependence of q_{EA} agrees with a random-

field smearing of a random-bond-type pseudo-spin-glass transition in the limit of fast motion. The parameters $\tilde{\Delta}$ and T_g of the proton-glass RTIDP are determined from the second moment of an ^{17}O NQR line as $\tilde{\Delta}=0.4$ and $T_g=210$ K.

-
- ¹E. Courtens, *J. Phys. (Paris) Lett.* **43**, L199 (1982).
²E. Courtens, *Ferroelectrics* **72**, 229 (1987).
³R. Blinc, J. Dolinšek, R. Pirc, B. Tadić, and B. Zalar, *Phys. Rev. Lett.* **63**, 2248 (1989).
⁴R. Pirc, B. Tadić, and R. Blinc, *Phys. Rev. B* **36**, 8607 (1987).
⁵R. Kind, R. Blinc, J. Dolinšek, N. Korner, B. Zalar, P. Cevc, N. S. Dalal, and J. Delooze, *Phys. Rev. B* **43**, 2511 (1991).
⁶Y. Ono, T. Hikita, and T. Ikeda, *J. Phys. Soc. Jpn.* **56**, 577 (1987).
⁷Y. Ono, T. Hikita, and T. Ikeda, *Ferroelectrics* **79**, 327 (1988).
⁸Y. Odden, A. Tranquard, and G. Pepe, *Acta Crystallogr. B* **35**, 542 (1979).
⁹R. J. Nelmes and R. N. P. Choudhary, *Solid State Commun.* **38**, 321 (1981).
¹⁰J. Seliger, V. Žagar, R. Blinc, and V. H. Schmidt, *J. Chem. Phys.* **88**, 3260 (1988).
¹¹N. S. J. Kennedy and R. J. Nelmes, *J. Phys. C* **13**, 4841 (1980).
¹²J. Seliger, V. Žagar, R. Blinc, and V. H. Schmidt, *Phys. Rev. B* **42**, 3881 (1990).
¹³R. Blinc, D. E. O'Reilly, E. M. Petersson, and J. M. Williams, *J. Chem. Phys.* **50**, 5408 (1969).
¹⁴A. I. Baranov, V. A. Sandler, L. A. Shuvalov, and R. M. Fedosyuk, *Ferroelectr. Lett.* **5**, 119 (1986).
¹⁵J. Grunberg, S. Levin, I. Pelah, and D. Gerlich, *Phys. Status Solidi B* **49**, 857 (1972).
¹⁶J. Seliger, V. Žagar, and R. Blinc, *Phys. Rev. B* **47**, 14753 (1993).
¹⁷R. E. Slusher and E. L. Hahn, *Phys. Rev.* **166**, 332 (1968).
¹⁸S. R. Hartmann and E. L. Hahn, *Phys. Rev.* **128**, 2042 (1962).
¹⁹N. Korner and R. Kind, *Phys. Rev. B* **49**, 5918 (1994).
²⁰R. Kind, R. Blinc, and M. Koren, *Phys. Rev. B* **37**, 4864 (1988).
²¹R. J. Nelmes, *Solid State Commun.* **39**, 741 (1981).
²²R. Blinc, S. Južnič, V. Rutar, J. Seliger, and S. Žumer, *Phys. Rev. Lett.* **44**, 609 (1980).
²³R. Blinc, J. Seliger, R. Osredkar, and M. Mali, *Phys. Lett. A* **47**, 131 (1974).
²⁴S. G. P. Brosnan and D. T. Edmonds, *Phys. Lett. A* **81**, 243 (1981).
²⁵J. Seliger, V. Žagar, and R. Blinc, *Phys. Lett. A* **93**, 149 (1983).
²⁶J. Seliger, V. Žagar, and R. Blinc, *J. Chem. Phys.* **81**, 3247 (1984).